Istraživanja i projektovanja za privredu
ISSN 1451-4117
DOI:10.5937/jaes0-66757
www.engineeringscience.rs

iipp publishing

Journal of Applied Engineering Science
Original Scientific Paper,
Volume 24, Number 4, Year 2026,
no 1365, pp 705-714

FIRE PERFORMANCE OF UNIFORM AND GRADED THIN-WALLED SQUARE STEEL COLUMNS

Qusay Al-Kaseasbeh*

Mutah University, Faculty of Engineering, Department of Civil and Environmental Engineering, Al-Karak, Jordan
**qusay.alkaseasbeh@mutah.edu.jo*

This study investigates the fire performance of uniform and graded thin-walled square steel columns under Hydrocarbon fire conditions. A sequentially coupled FE model in ABAQUS is employed to assess the effect of wall thickness (9 mm and 13 mm), thickness grading, longitudinal stiffeners, and diaphragm systems under a constant axial load ratio of 10% of squash load. A total of 28 configurations is analysed for both thicknesses, including uniform and graded square sections with and without internal reinforcement (i.e., stiffeners and/or Diaphragms). Structural performance is evaluated using developed compressive axial force, buckling time resistance (BTR) and failure time resistance (FTR). The results reveal that increasing wall thickness significantly improves fire performance, with normalized improvements of up to 135%, 56%, and 88% in compressive axial force, BTR, and FTR, respectively. Moreover, thickness grading consistently enhances both BTR and FTR, with clear advantages observed at higher thickness. Longitudinal stiffeners are identified as the most effective strengthening technique, while the benefits of grading within stiffeners diminishes as thickness increases. In contrast, diaphragms contribute insignificantly to structural performance. These findings indicate that fire response of thin-walled square steel columns is governed by local plate buckling, and stiffeners are being effective than diaphragms reinforcement.

Keywords: steel, square, hydrocarbon fire, thickness grading, buckling, stiffened columns

HIGHLIGHTS

- FE numerical models were constructed to study graded thin-walled square steel columns exposed to hydrocarbon fire.
- Thickness grading improved BTR and FTR without increasing material volume.
- Longitudinal stiffeners provided the greatest enhancement in axial capacity and fire resistance.
- Diaphragms had negligible influence, confirming that local plate buckling governs fire response

NOMENCLATURE

FE	Finite Element	SU	Uniform Stiffeners
BTR	Buckling Time Resistance	SG	Graded Stiffeners
FTR	Failure Time Resistance	DU	Uniform Diaphragms
UB	Uniform Section	DG	Graded Diaphragms
GB	Graded Section		

1 Introduction

Owing to their efficient structural behavior and high strength-to-weight ratio, thin-walled steel columns are extensively used in modular structures, offshore and onshore platforms, and particularly in bridge systems as piers [1–6]. Nevertheless, their response under hydrocarbon fire is still a major concern. Such structures are prone to early buckling due to their large surface area, which heats up quickly and lead to stiffness degradation and structural instability [4, 5, 7–10]. The fire performance of steel structures of uniform cross-sections has been extensively investigated [11], but advanced configurations, such as internally reinforced or graded cross sections, have received limited attention [12, 13]. Structural steel response under fire is governed by material degradation, thermal expansion, and buckling [12]. Numerous numerical and experimental studies have proven that fire resistance of such steel columns are significantly affected by their height, slenderness ratio, and axial load ratio at elevated temperatures [14]. The plate local instability dominates the structural performance of thin-walled cold formed steel structures. Thin-walled structures are sensitive to local buckling under fire exposure [15], and slenderness of the cross-section plays a role in failure mode of such structures [16, 17]. These findings emphasized the need for enhancing the local stability to improve the fire resistance of these structures. At elevated fire temperatures, the steel stiffness progressively reduces and increases the susceptibility of the column to the local buckling [18].

Several practices have been proposed to improve the local buckling, including longitudinal stiffener and diaphragms, which are used to reduce the plate slenderness and control the local buckling phenomenon [8]. Longitudinal stiffeners reduce the slenderness and effective width of the column's plates, which improves the resistance to the local buckling [19]. However, their efficiency has not been evaluated under hydrocarbon fire exposure. In parallel, Al-Kaseasbeh et al. [1, 20–22] proposed thickness grading configuration as an effective optimization approach to improve the ductility

and buckling resistance of thin-walled steel structures under cyclic loading, which improves the stress distribution and delay the initiation of local buckling. These studies shown that redistributing the material along the column can improve structural behavior without necessarily increasing the total material volume. More recently, the fire behavior of corrugated thin-walled steel column have been investigated using validated FE models in ABAQUS, highlighting the effect of geometrical configuration and material distribution on fire resistance [12]. Despite these advantages, the performance of graded thin-walled square steel cross sections under hydrocarbon fire has not been sufficiently studied, practically when stiffeners and diaphragms are included. Furthermore, the combined effect of thickness grading, longitudinal stiffeners, and diaphragms on the fire response of thin-walled square steel columns has not been systematically investigated. This limited understanding of the combined effect of thickness grading, stiffeners, and diaphragms represents a critical research gap to evaluate the performance of thin-walled square steel cross sections under hydrocarbon fire exposure. Additional details of validated FE model are thoroughly provided in a previous study by the author [13].

Therefore, this FE study aims to investigate the fire performance of thin-walled square steel columns exposed to hydrocarbon fire, by considering the combined influence of thickness grading, longitudinal stiffeners, and diaphragms. A validated FE model was used to evaluate the compressive axial force, buckling time resistance (BTR) and failure time resistance (FTR), and identify the most effective configuration for improving the fire performance of thin-walled square steel columns under hydrocarbon fire conditions.

2 Materials and methods

2.1 FE modeling approach

The performance of thin-walled square steel columns is simulated by a sequentially coupled thermal–structural ABAQUS finite element (FE) modelling under hydrocarbon fire exposure. The FE analysis is conducted in two consecutive steps. In the first step, a transient heat transfer analysis was carried out to calculate the fire temperature distribution within the steel cross-section over time. Then, the temperature field was imported into a FE nonlinear structural analysis to assess the thermal-structural behavior of the column. This strategy accurately represents the thermal-dependent steel materials degradation and its effect on the column stability. To ensure an efficient transfer between thermal and structural analyses, the step time increment, the consistent meshing discretization, and most importantly the same elements family should be adopted in both thermal and structural FE analyses [23]. In other words, heat transfer analysis is modeled using DS4 shell elements, whereas the S4R shell elements are employed for the structural analysis to ensure an efficient buckling behavior capture and be consistent with the validated FE model. Additional details of validated FE model are provided in a previous study by the author [13]. Under hydrocarbon fire conditions, a uniform fire exposure is assumed in outer surface along the whole height of the modeled column. Both convective and radiative heat transfer are considered in the thermal analysis [24]. Consistent Eurocode recommendations, the emissivity, convection coefficient, and Stefan–Boltzmann constant taken as 0.7, 50 W/(m²·°C), and 5.67 × 10^{-8} W/(m²·K⁴), respectively [25–28].

2.2 Geometry and models configuration

28 thin-walled square steel columns with a side length of L = 900 mm and a total height of h = 3403 mm were investigated in this FE study, see Fig. 1a. Two wall thicknesses, t = 9 mm and 13 mm, were examined to evaluate the effect of the column plate thickness on the fire performance. In the uniform configuration (UB), the wall thickness was kept same along the full height of the column. For graded configurations (GB), the column height was divided into three segments. The lower and middle segments were each assigned to a length equal to the side dimension of the section (900 mm), while the remaining upper segment had a length of h-2L. A thickness of 1.25t was assigned to the lower segment, while the original thickness kept to the middle segment, and calculating the thickness of the upper segment by maintaining the material volume conservation to facilitate a direct comparison without increasing the total mass of steel material. Longitudinal stiffeners, when included, were modeled as plates with a thickness of 6 mm and a width of 80 mm, uniformly distributed along the column sides at a spacing of 225 mm, see Fig 1a and b. Two stiffener configurations were analyzed: uniform stiffeners (SU), in which the stiffener thickness maintained constantly along the column height, and graded stiffeners (SG), in which the stiffeners were segmented consistently with the square section grading. For the graded stiffeners, a thickness of 1.25ts was assigned to the lower segment, the original thickness ts was for the middle segment, and the thickness of the upper segment was calculated to maintain constant material volume of the stiffener. Diaphragms were modeled as transverse plates located at predefined positions along the column height (900 and 1800 mm from the base), see Fig. 1c. In the uniform diaphragm configuration (DU), a constant thickness was used for all diaphragms. In the graded diaphragm configuration (DG), the thickness of the first diaphragm from the base was increased to 1.25td, while the thickness of the subsequent diaphragm was maintained at td. A total of 28 models were analyzed, including uniform and graded square sections with and without stiffeners and diaphragms, in addition to combined configurations. All graded configurations were constructed under a constant material volume, ensuring that any observed improvement in fire performance is only attributed to the material distribution not an increase in material volume. This systematic configuration and thicknesses matrix, shown in Tables 1 and 2, facilitates a comprehensive evaluation of the individual and combined effects of thickness grading, stiffeners, and diaphragms on the fire performance of thin-walled square steel columns.

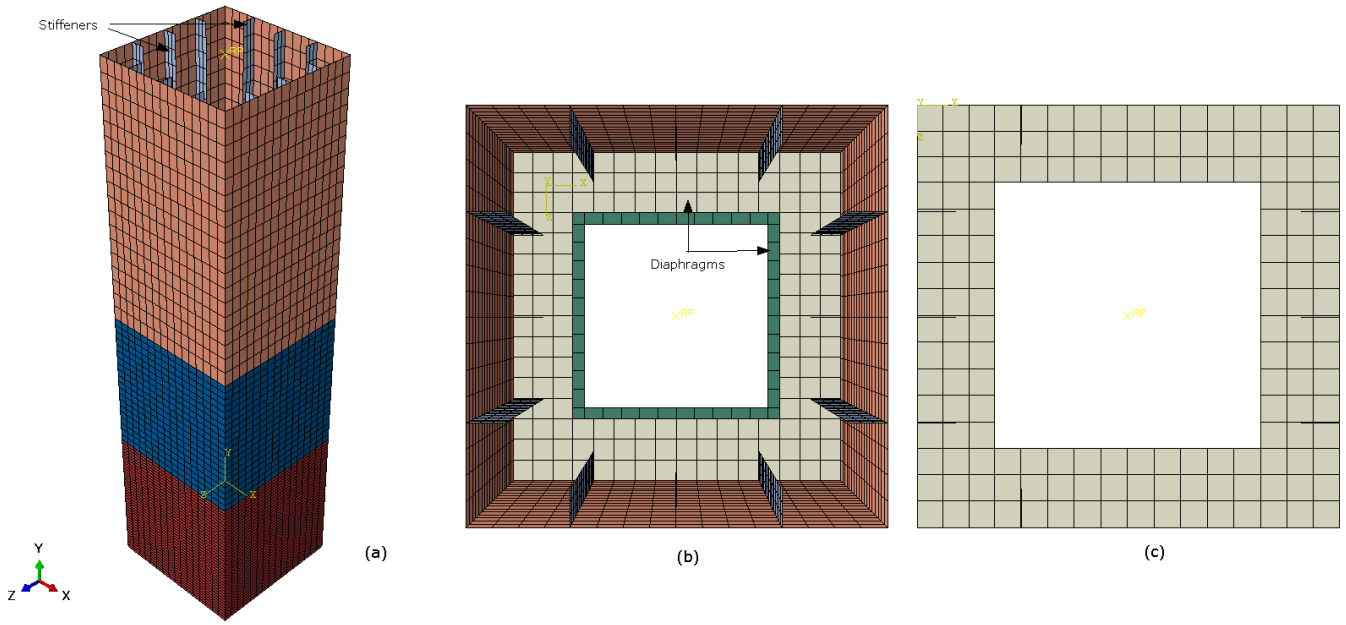


Fig. 1. Column configuration: (a) FE Geometry, (b) Cross-section, (c) Diaphragm Section

Table 1. Configuration matrix for FE study under hydrocarbon fire

Case ID	Box Section	Stiffeners	Diaphragms
UB	Uniform	None	None
GB	Graded	None	None
UB-SU	Uniform	Uniform	None
GB-SU	Graded	Uniform	None
UB-SG	Uniform	Graded	None
GB-SG	Graded	Graded	None
UB-DU	Uniform	None	Uniform
GB-DU	Graded	None	Uniform
UB-DG	Uniform	None	Graded
GB-DG	Graded	None	Graded
UB-SU-DU	Uniform	Uniform	Uniform
GB-SU-DU	Graded	Uniform	Uniform
UB-SG-DG	Uniform	Graded	Graded
GB-SG-DG	Graded	Graded	Diaphragms

Table 2. Thickness matrix for FE study under hydrocarbon fire

Component	Uniform thickness (t)	Lower segment (1.25t)	Middle segment (t)	Upper segment
Thickness (9 mm)	9	11.25	9	7.75
Thickness (13 mm)	13	16.25	13	11.2
Stiffener (ts)	6	7.5	6	5.16
Diaphragm (td)	6	7.5	6	—

2.3 Material properties and fire curve

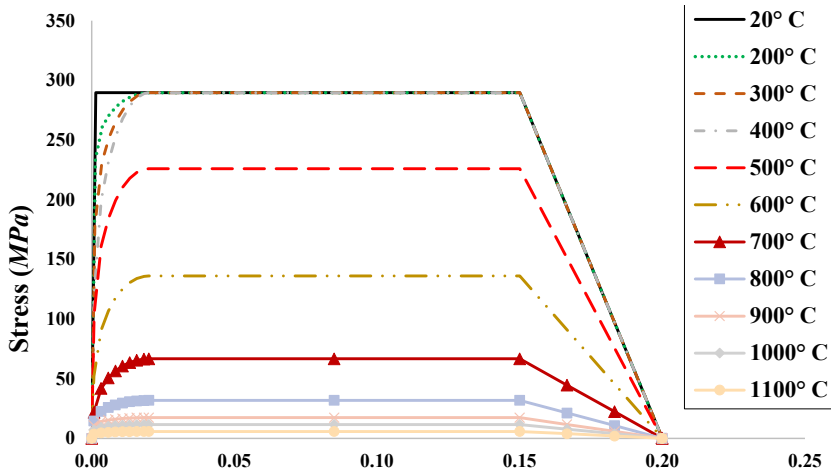


Fig. 2. Stress-strain relationship for carbon steel at elevated temperatures [12, 29]

The steel material behavior was defined using temperature-dependent relationships in Eurocode 3 Part 1-2 [29]. The degradation of mechanical properties at elevated temperatures was incorporated into the model to accurately represent the progressive loss of stiffness and strength as temperature increases under fire conditions. A constant axial load corresponding to 10% of the squash load at ambient temperature applied to the top of the investigated column. Then, hydrocarbon fire curve was applied, which is representative of extreme fire conditions usually encountered in petrochemical accidents, as shown in Fig. 2. Heat transfer was modeled by convection and radiation within the column and applied to simulate the exchange of heat from the fire to column surface. Initially, transient heat analysis was performed to evaluate the temperature distribution within the column over time. Then, the temperature output was incorporated into the structural analysis. This sequentially coupled analysis simulates the interaction between thermal loading and structural performance and captures the effect of temperature evolution on instability under hydrocarbon fire. All FE analyzed columns are assumed to be ASTM A36 steel [30] with a yield stress of 289.6 MPa and an elastic modulus of 206 GPa [8].

2.4 Boundary conditions, and FE meshing

The analyzed columns were subjected to a constant axial load corresponding to 10% of the squash load at ambient temperature. Boundary conditions were modeled to simulate realistic column supports. The base of the column was fixed, whereas the top end was permitted to displace axially under the applied load to allow axial deformation and local instability. The columns were meshed using shell elements proper for modeling thin-walled sections (i.e., S4R elements for structural analysis and DS4 elements for thermal analysis). A refined mesh was gradually employed along the column height to capture local buckling behavior, and temperature gradients, see Fig 1. An element sizes of 22.5, 45, and 90 mm adopted in the lower, middle, and upper mesh regions, respectively. Across the cross-section, the region between adjacent longitudinal stiffeners was discretized into four elements, while the width of each stiffener was divided into three elements. The mesh along the stiffener length were meshed consistently with the corresponding column mesh. Similarly, the diaphragm mesh was compatible with the column mesh at its location. Special attention was given to regions expected to experience high thermal and mechanical gradients, such as near the base and within graded segments.

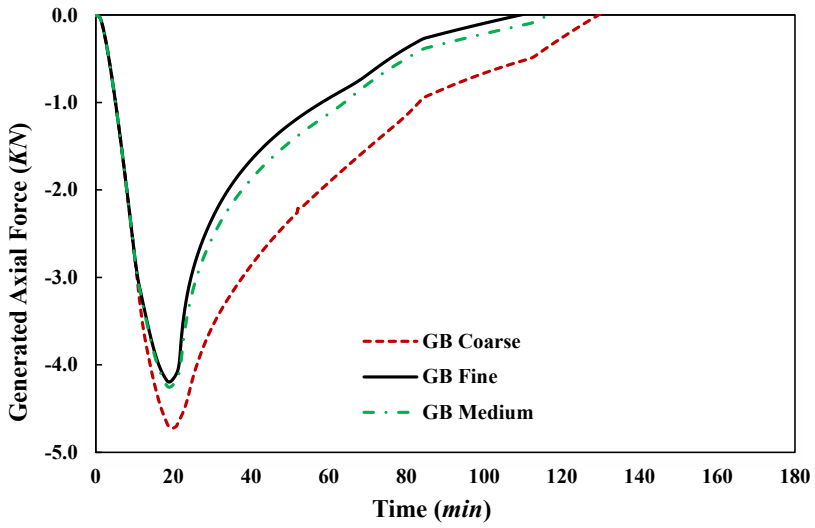


Fig. 3. Mesh-convergence analysis of the GB column with 9 mm

A mesh-convergence analysis was carried out for the GB column as a representative FE model. Three mesh densities, namely coarse, medium, and fine, were considered. The medium mesh, which was adopted for parametric study, had element sizes of 22.5, 45, and 90 mm in the corresponding mesh regions. For the coarse mesh, these element sizes were doubled to 45, 90, and 180 mm, respectively, whereas for the fine mesh, they were reduced by half to 11.25, 22.5, and 45 mm. Fig 3 compares the generated axial force capacity for the three mesh densities. The coarse mesh shows a noticeable difference, specifically around the maximum compressive axial force and the subsequent response, whereas the medium and fine meshes show close agreement. The computational time was less than approximately 1 min for the coarse mesh and about 4 min for the medium mesh, while the fine mesh required substantially longer computational time. Since further mesh refinement produced only a minor change in the predicted response at a considerably higher computational cost, the medium mesh was adopted for parametric study as an appropriate balance between numerical accuracy and computational efficiency.

2.5 Failure parameters

The steel column initially develops a compressive axial force due to the restraint against thermal expansion under hydrocarbon exposure [31, 32]. As the fire temperature increases, the stiffness and rigidity of the steel column decreases, which triggers the onset of the local buckling and rapid deformation increase. Then, the developed compressive axial force decreases gradually and eventually shifted to the tensile force phase [33].

In the current study, the column performance is evaluated with three indicators. The maximum compressive axial force represents the load-carrying capacity of the steel column. The buckling time resistance (BTR) is defined as the fire resistance corresponding to the maximum compressive axial force, indicating the initiation of buckling. The failure time resistance (FTR) is defined at which the zero-axial generated compressive force is reached, marking the complete loss of the load-carrying capacity of the heated column [13], see Fig 4. Moreover, the duration of the hydrocarbon fire exposure of 180 minutes was adopted in the current study, which is commonly used in the fire resistance testing [34, 35].

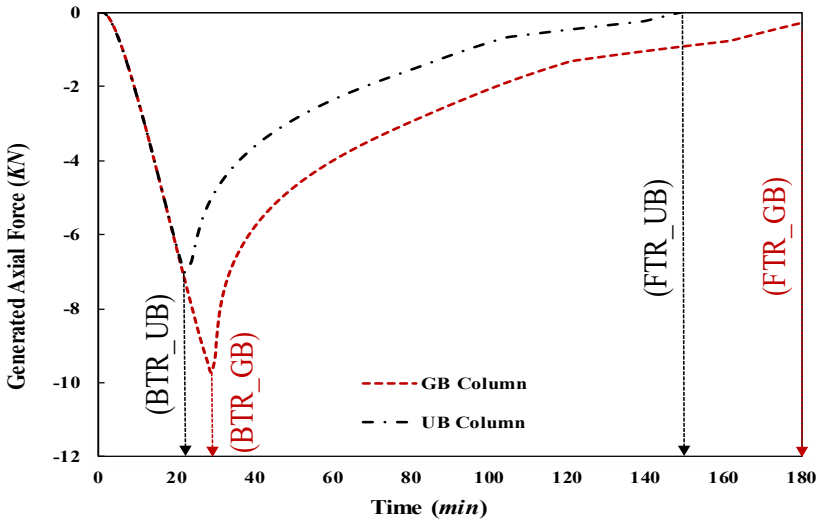


Fig. 4. Generated compressive axial force history indicating BTR and FTR indicators for 13 mm

3 Results and discussion

3.1 Effect of wall thickness

As shown in Fig. 5, Increasing the wall thickness from 9 mm to 13 mm resulted in a significant improvement in axial force for all configurations. The axial force improved by 42% to 134%, depending on the section configuration. The biggest improvements observed in unstiffened systems, such as UB column and diaphragm-only configurations (UB-DU and UB-DG), were the axial force more than doubled, reaching increases of up to 134%. In contrast, stiffened configurations show less improvements, in the range of 42% to 47%, indicating that stiffeners reduce the sensitivity of the column to thickness variation. This behavior confirms that increasing thickness significantly improves plate stiffness and resistance to local buckling.

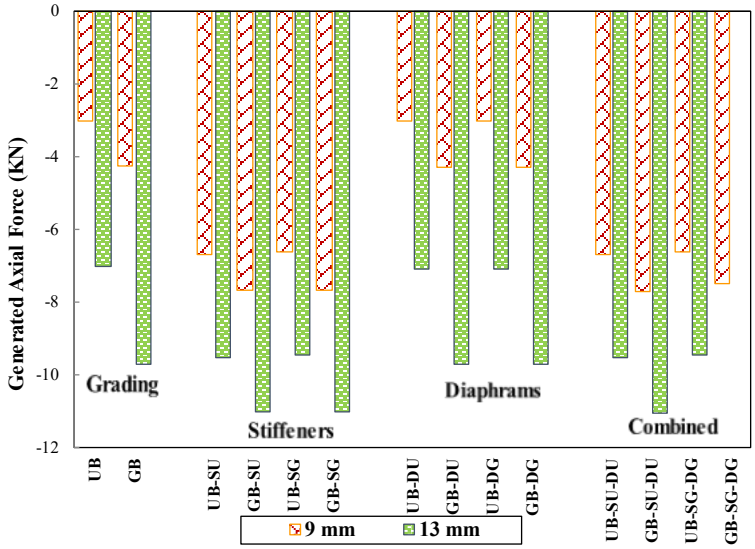


Fig. 5. Maximum axial force capacity for all configurations

3.2 Effect of thickness grading

Thickness grading of the column consistently enhanced structural response across all parameters (BTR, FTR, and axial force). The maximum increase in BTR is 31% for graded configurations compared to uniform sections, indicating a more effective delay in the local buckling, see Fig. 6 (Left). In addition, a significant improvement in FTR achieved, with approximately 50% in configurations without stiffeners, see Fig. 6 (Right).

In a similar trend, the axial force of graded sections showed clear improvement compared to uniform configurations. In unstiffened configurations, the axial force increased by more than 42%, indicating that thickness grading significantly improves axial force by delaying local buckling. In contrast, for stiffened systems, the increase in axial force was less, about 16% indicating that the presence of stiffeners reduces the contribution of grading, see Fig. 5. In addition, thickness grading shows minimal effect on axial deformation, with improvements generally remaining below 5%.

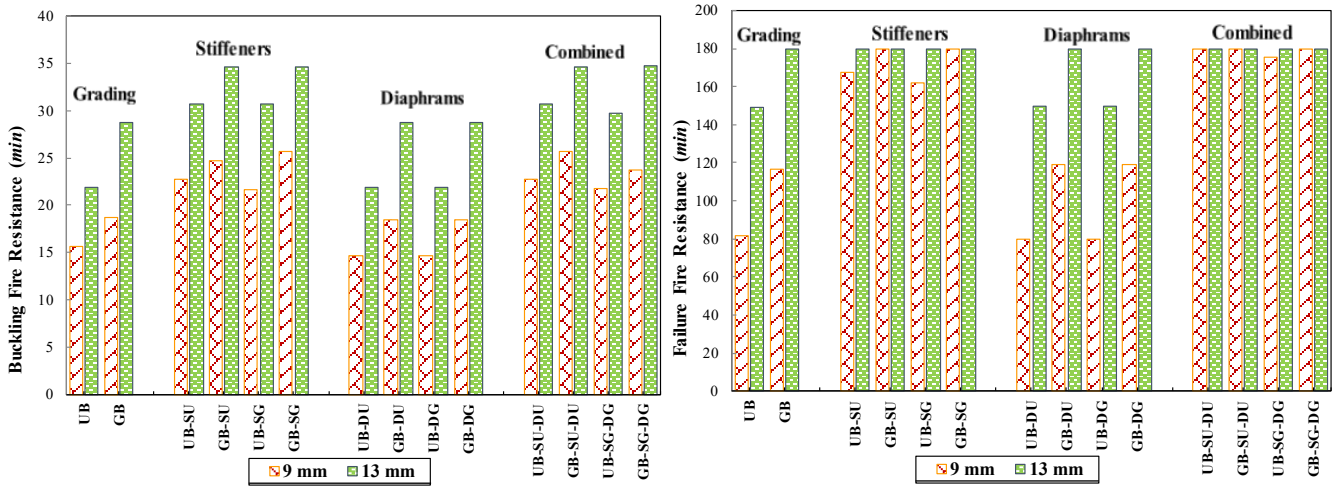


Fig. 6. Comparison of Fire indicators: BTR (Left) and FTR (Right) for all configurations

3.3 Effect of longitudinal stiffeners

The inclusion of longitudinal stiffeners substantially improved the structural performance across all indicators, including BTR, FTR, axial force, see Figs 5 and 6. Stiffeners reduce plate slenderness, thereby delaying the initiation of local buckling and improving overall stability. This effect is reflected in the increase in BTR, where stiffened configurations show improvements in the range of 32% to 45%, indicating a delay of buckling. Similarly, the FTR shows moderate enhancement in stiffened configurations. In terms of axial force, stiffeners contribute significantly to improvement of structural strength, approximately 81% to 121% compared to increases of 40% in unstiffened sections. This indicates that stiffeners contributed to stabilizing of the columns, thereby reducing the sensitivity of the column to thickness increase. Moreover, the effect of thickness grading within stiffeners diminishes at higher thickness values. The difference between graded and uniform stiffener configurations becomes less effective with approximately improvement of 13% to 36%, suggesting that once sufficient stiffness is achieved, further optimization of material distribution has limited impact on overall performance.

3.4 Effect of diaphragms

As shown in Fig. 5, diaphragm inclusion showed no substantial effect on the structural behavior across all indicators. The improvements in BTR and FTR for diaphragm configurations were comparable to those of unstiffened columns, indicating that diaphragms do not contribute to delaying buckling or enhancing the fire resistance. Similarly, the axial force exhibited no improvement due to diaphragm inclusion. This indicates that diaphragms do not effectively contribute to improving axial force under hydrocarbon fire exposure. Even when combined with thickness grading, diaphragms did not provide remarkable improvements. This suggests that diaphragms are not effective in limiting local buckling, which governs the structural response under fire exposure. Therefore, their contribution to fire performance seems to be limited.

3.5 Buckling modes

Fig. 7 demonstrates the buckling mode of selected column configurations at the end of the analysis at hydrocarbon fire exposure. Comparing the UB and GB columns exhibits that thickness grading changes the distribution and location of deformation. The UB column shows more localized deformation, especially around the transition region between the lower and middle segments, whereas the GB column develops a more distributed deformation pattern along the column height. This indicates that thickness grading redistributes the deformation and reduces its localization. The comparison between GB-SG and GB-DU configurations further shows the effect of the internal reinforcement. The GB-SG column shows a more distributed deformation with less pronounced localization, indicating the effectiveness of longitudinal stiffeners in controlling local deformation of the column plates. In contrast, GB-DU exhibits a deformation pattern closer to the GB column, reflecting that the diaphragms have a limited influence on controlling the governing buckling mode. These observations are consistent with the BTR, FTR, and axial-force results, which showed a greater contribution from longitudinal stiffeners than from diaphragms.

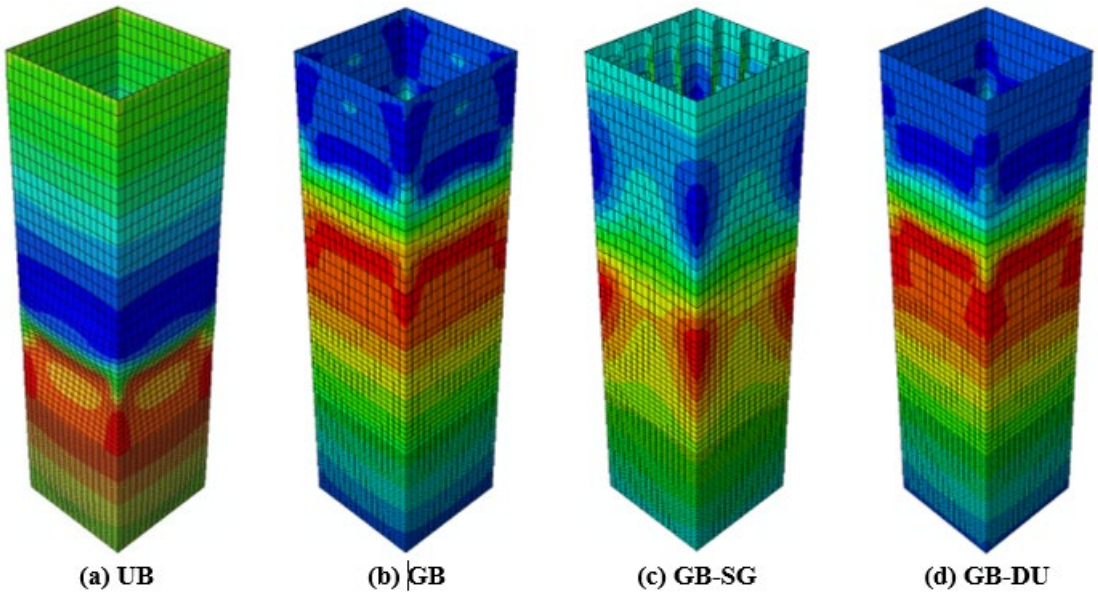


Fig. 7. Buckling modes of selected column: (a) UB, (b) GB, (c) GB-SG, and (d) GB-DU

4 Conclusions

The fire performance of uniform and graded thin-walled square steel columns has been numerically investigated under hydrocarbon fire exposure. The effect of wall thickness, thickness grading, longitudinal stiffeners, and diaphragms has been considered. Based on the FE results and within the range investigated parameters considered in the current study, the following conclusions are summarized:

- Wall thickness has a dominant effect on structural behavior under hydrocarbon fire. Increasing thickness from 9 mm to 13 mm significantly improves axial force capacity, BTR, and FTR indicators for the investigated column configurations.
- Thickness grading is confirmed to be an effective strategy to improve the fire performance within the column configurations investigated. Graded configurations achieve up to 31% improvement in BTR and approximately 50% increase in FTR. Axial force is also enhanced, particularly in unstiffened columns, while the relative benefit of grading becomes less significant in the presence of stiffeners.
- For the stiffeners configurations included in the current study, longitudinal stiffeners significantly improve the axial force by approximately 81%–121 and improve BTR by 32%–45%. The inclusion of stiffeners reduces the sensitivity of the system to both thickness increase and grading.

- Diaphragms have ineffective improvement on fire response or governing the local buckling. No meaningful enhancement was observed in axial force, BTR, or FTR, even when combined with thickness grading under hydrocarbon fire for the diaphragm locations and arraignments investigated in the current study.
- Axial deformation exhibits minimal influence across all investigated column configurations. Despite significant improvements in strength and fire resistance, deformation remains within 5% or less, indicating that it is not the governing parameter in the structural performance for the configurations considered in the current study.

5 Acknowledgment

The author sincerely acknowledges the continuous support provided by Mutah University.

6 References

[1] Al-Kaseasbeh, Q., & Mamaghani, I. H. P. (2019). Design and cyclic elastoplastic analysis of graded thin-walled steel tubular columns with enhanced strength and ductility. *International Journal of Modern Engineering, 19*(1), 30–36.

[2] Al-Kaseasbeh, Q., & Mamaghani, I. H. P. (2019). Thin-walled steel tubular circular columns with uniform and graded thickness under bidirectional cyclic loading. *Thin-Walled Structures, 145*, 106449. https://doi.org/10.1016/j.tws.2019.106449

[3] Al-Kaseasbeh, Q., & Mamaghani, I. H. P. (2019). Performance of thin-walled steel tubular circular columns with graded thickness under bidirectional cyclic loading. In *Structures Congress 2019: Bridges, Tunnels, and Other Transportation Structures* (pp. 1–10). American Society of Civil Engineers. https://doi.org/10.1061/9780784482230.001

[4] Ucak, A., & Tsopelas, P. (2015). Load path effects in circular steel columns under bidirectional lateral cyclic loading. *Journal of Structural Engineering, 141*(5), 04014133. https://doi.org/10.1061/(ASCE)ST.1943-541X.0001057

[5] Bedair, O. (2015). Novel design procedures for rectangular hollow steel sections subject to compression and major and minor axis bending. *Practice Periodical on Structural Design and Construction, 20*(4), 04014051. https://doi.org/10.1061/(ASCE)SC.1943-5576.0000248

[6] Goto, Y., Mizuno, K., & Ghosh, P. K. (2012). Nonlinear finite element analysis for cyclic behavior of thin-walled stiffened rectangular steel columns with in-filled concrete. *Journal of Structural Engineering, 138*(5), 571–584. https://doi.org/10.1061/(ASCE)ST.1943-541X.0000504

[7] Al-Kaseasbeh, Q., & Mamaghani, I. H. P. (2019). Buckling strength and ductility evaluation of thin-walled steel stiffened square box columns with uniform and graded thickness under cyclic loading. *Engineering Structures, 186*, 498–507. https://doi.org/10.1016/j.engstruct.2019.02.026

[8] Al-Kaseasbeh, Q., & Mamaghani, I. H. P. (2020). Thin-walled steel stiffened square box columns with uniform and graded thickness under bidirectional cyclic loading. *Engineering Structures, 219*, 110919. https://doi.org/10.1016/j.engstruct.2020.110919

[9] Albarram, A., & Al-Kaseasbeh, Q. (2025). Analysis of perforated corrugated steel columns subjected to bilateral cyclic loading. *International Journal of Protective Structures, 16*(2), 319–339. https://doi.org/10.1177/20414196241235321

[10] Yang, C., Zhao, H., Sun, Y., & Zhao, S. (2017). Compressive stress-strain model of cold-formed circular hollow section stub columns considering local buckling. *Thin-Walled Structures, 120*, 495–505. https://doi.org/10.1016/j.tws.2017.09.017

[11] Arya, C. (2009). *Design of structural elements: Concrete, steelwork, masonry and timber designs to British standards and Eurocodes* (3rd ed.). CRC Press.

[12] Al-Kaseasbeh, Q. (2024). Investigating the fire resistance of corrugated steel columns. *Results in Engineering, 21*, 101687. https://doi.org/10.1016/j.rineng.2023.101687

[13] Al-Kaseasbeh, Q. (2023). Analysis of hydrocarbon fire-exposed cold-formed steel columns. *Results in Engineering, 20*, 101400. https://doi.org/10.1016/j.rineng.2023.101400

[14] Fan, S., Ding, X., Sun, W., Zhang, L., & Liu, M. (2016). Experimental investigation on fire resistance of stainless steel columns with square hollow section. *Thin-Walled Structures, 98*, 196–211. https://doi.org/10.1016/j.tws.2015.02.003

[15] Schafer, B. W. (2008). Review: The direct strength method of cold-formed steel member design. *Journal of Constructional Steel Research, 64*(7–8), 766–778. https://doi.org/10.1016/j.jcsr.2008.01.022

[16] Ermopoulos, J., & Spyrakos, C. C. (2006). Validated analysis and strengthening of a 19th century railway bridge. *Engineering Structures, 28*(5), 783–792. https://doi.org/10.1016/j.engstruct.2005.10.006

[17] Gardner, L., & Ashraf, M. (2006). Structural design for non-linear metallic materials. *Engineering Structures, 28*(6), 926–934. https://doi.org/10.1016/j.engstruct.2005.11.001

[18] Kamil, G. M., Liang, Q. Q., & Hadi, M. N. S. (2018). Local buckling of steel plates in concrete-filled steel tubular columns at elevated temperatures. *Engineering Structures, 168*, 108–118. https://doi.org/10.1016/j.engstruct.2018.04.073

[19] Luo, K., Li, H., Yang, J., Fang, S., Yan, F., Yu, J., Han, X., Xu, Y., & Ning, X. (2025). Research on post-fire cold-formed steel back-to-back built-up columns with local buckling. *Thin-Walled Structures, 209*, 112883. https://doi.org/10.1016/j.tws.2024.112883

[20] Al-Kaseasbeh, Q., & Mamaghani, I. H. P. (2018). Buckling strength and ductility evaluation of thin-walled steel tubular columns with uniform and graded thickness under cyclic loading. *Journal of Bridge Engineering, 24*(1), 04018105. https://doi.org/10.1061/(ASCE)BE.1943-5592.0001324

[21] Al-Kaseasbeh, Q. A. (2019). *Hysteretic behavior of thin-walled steel tubular columns under constant axial force and cyclic lateral loading* [Doctoral dissertation, University of North Dakota]. University of North Dakota Scholarly Commons. https://commons.und.edu/theses/2442

[22] Al-Kaseasbeh, Q. (2021). Comparative numerical study of circular-shaped steel tubes subjected to cyclic horizontal loading. In *Proceedings of the 1st International Conference on Structural Damage Modelling and Assessment: SDMA 2020* (pp. 167–175). Springer. https://doi.org/10.1007/978-981-15-9121-1_13

[23] Lu, H., Zhao, X. L., & Han, L. H. (2011). FE modelling and fire resistance design of concrete filled double skin tubular columns. *Journal of Constructional Steel Research, 67*(11), 1733–1748. https://doi.org/10.1016/j.jcsr.2011.04.014

[24] Zhang, G., Kodur, V., Song, C., He, S., & Huang, Q. (2020). A numerical model for evaluating fire performance of composite box bridge girders. *Journal of Constructional Steel Research, 165*, 105823. https://doi.org/10.1016/j.jcsr.2019.105823

[25] Song, C., Zhang, G., Hou, W., & He, S. (2020). Performance of prestressed concrete box bridge girders under hydrocarbon fire exposure. *Advances in Structural Engineering, 23*(8), 1521–1533. https://doi.org/10.1177/1369433219898102

[26] European Committee for Standardization. (2002). *EN 1991-1-2: Eurocode 1: Actions on structures—Part 1-2: General actions—Actions on structures exposed to fire*. CEN.

[27] International Organization for Standardization. (1999). *ISO 834-1:1999: Fire-resistance tests—Elements of building construction—Part 1: General requirements*. ISO.

[28] ASTM International. (2006). *ASTM E1529-06: Standard test methods for determining effects of large hydrocarbon pool fires on structural members and assemblies*. ASTM International.

[29] European Committee for Standardization. (2005). *Eurocode 3: Design of steel structures—Part 1-2: General rules—Structural fire design*. CEN.

[30] ASTM International. (2014). *ASTM A36/A36M-14: Standard specification for carbon structural steel*. ASTM International. https://doi.org/10.1520/A0036_A0036M-14

[31] Wang, P., Wang, Y. C., & Li, G. Q. (2010). A new design method for calculating critical temperatures of restrained steel column in fire. *Fire Safety Journal, 45*(6–8), 349–360. https://doi.org/10.1016/j.firesaf.2010.07.002

[32] Wang, Y., Mahendran, M., & Shahbazian, A. (2020). *Fire performance of thin-walled steel structures*. CRC Press. https://doi.org/10.1201/9781351011815

[33] Iqbal, N., Heistermann, T., Veljkovic, M., Lopes, F., Santiago, A., & da Silva, L. S. (2016). Axial force and deformation of a restrained steel beam in fire: Description and validation of a simplified analytical procedure. *Advanced Steel Construction, 12*(2), 174–193. https://doi.org/10.18057/IJASC.2016.12.2.6

[34] Gravit, M., Dmitriev, I., Shcheglov, N., & Radaev, A. (2024). Oil and gas structures: Forecasting the fire resistance of steel structures with fire protection under hydrocarbon fire conditions. *Fire, 7*(6), 173. https://doi.org/10.3390/fire7060173

[35] International Organization for Standardization. (2025). *ISO 834-1:2025: Fire-resistance tests—Elements of building construction—Part 1: General requirements*. ISO.

7 Conflict of interest statement

The author declares no conflict of interest.

8 Author contributions

Qusay Al-Kaseasbeh contributed to the conceptualization, methodology, finite element modeling, numerical analysis, data analysis, visualization, and preparation and revision of the manuscript. The author has read and approved the final manuscript.

9 Data availability statement

The data supporting the findings of this study are available from the corresponding author upon request.

10 Supplementary materials

There are no supplementary materials associated with this study.

Paper submitted: 22.06.2026.
Paper accepted: 14.08.2026.
This is an open access article distributed under the CC BY 4.0 terms and conditions